HHS Public Access

Author manuscript

Toxicol Appl Pharmacol. Author manuscript; available in PMC 2019 March 04.

Published in final edited form as:

Toxicol Appl Pharmacol. 2017 August 15; 329: 1–8. doi:10.1016/j.taap.2017.05.015.

Impact of hepatic P450-mediated biotransformation on the disposition and respiratory tract toxicity of inhaled naphthalene

Nataliia Kovalchuk[1], **Jacklyn Kelty**[2], **Lei Li**[1], **Matthew Hartog**[3], **Qing-Yu Zhang**[1], **Patricia Edwards**[2], **Laura Van Winkle**[2,*], and **Xinxin Ding**[3,*]

[1]Wadsworth Center, New York State Department of Health, and School of Public Health, State University of New York at Albany, NY 12201

[2]UC Davis, Davis, CA 95616

[3]College of Nanoscale Science, SUNY Polytechnic Institute, Albany, NY 12203

Abstract

We determined whether a decrease in hepatic microsomal cytochrome P450 activity would impact lung toxicity induced by inhalation exposure to naphthalene (NA), a ubiquitous environmental pollutant. The liver-Cpr-null (LCN) mouse showed decreases in microsomal metabolism of NA in liver, but not lung, compared to wild-type (WT) mouse. Plasma levels of NA and NA-glutathione conjugates (NA-GSH) were both higher in LCN than in WT mice after a 4-h nose-only NA inhalation exposure at 10 ppm. Levels of NA were also higher in lung and liver of LCN, compared to WT, mice, following exposure to NA at 5 or 10 ppm. Despite the large increase in circulating and lung tissue NA levels, the level of NA-GSH, a biomarker of NA bioactivation, was either not different, or only slightly higher, in lung and liver tissues of LCN mice, relative to that in WT mice. Furthermore, the extent of NA-induced acute airway injury, judging from high-resolution lung histopathology and morphometry at 20 h following NA exposure, was not higher, but lower, in LCN than in WT mice. These results, while confirming the ability of extrahepatic organ to bioactivate inhaled NA and mediate NA's lung toxicity, suggest that liver P450-generated NA metabolites also have a significant, although relatively small, contribution to airway toxicity of inhaled NA. This hepatic contribution to the airway toxicity of inhaled NA may be an important risk factor for individuals with diminished bioactivation activity in the lung.

Keywords

naphthalene; metabolism; inhalation; lung; airway; toxicity; liver; P450

[*]Corresponding authors: X. Ding (xding@sunypoly.edu) and L. Van Winkle (lsvanwinkle@ucdavis.edu). **Address Manuscript Correspondence To:** Dr. Xinxin Ding, 257 Fuller Rd., College of Nanoscale Science, SUNY Polytechnic Institute, Albany, NY 12203. Tel. 518-588-5478; xding@sunypoly.edu.
Address Manuscript Correspondence To: Dr. Xinxin Ding, 257 Fuller Rd., College of Nanoscale Science, SUNY Polytechnic Institute, Albany, NY 12203., Tel. 518-588-5478; xding@sunypoly.edu

Conflict of Interest Statement
The authors declare that there are no conflicts of interest.

INTRODUCTION

Naphthalene (NA) is a ubiquitous contaminant of the environment (USEPA, 1986; Witschi *et al.*, 1997; Kakareka and Kukharchyk, 2003). NA is classified as a Possible Human Carcinogen (group 2B) (IARC, 2002), in part due to its ability to induce nasal tumors in rats and lung tumors in mice in chronic rodent bioassays conducted by the National Toxicology Program (Abdo *et al.*, 1992; Abdo *et al.*, 2001). The current OSHA standard for NA exposure in the workplace is 10 ppm. NA administration injures nonciliated bronchiolar epithelial cells (Club cells) in conductive airways independent of the route of administration in rodents (Plopper *et al.*, 1992a; Plopper *et al.*, 1992b; West *et al.*, 2001).

The mechanism of NA carcinogenicity is not fully understood; but it is clear that cytochrome P450 (P450)-mediated NA bioactivation is essential for NA toxicity, and repeated cycles of NA-induced acute cytotoxicity with subsequent tissue repair are believed to be important initiating events for NA carcinogenicity (Buckpitt *et al.*, 2002; Brusick, 2008). Bioactivation of NA to its reactive metabolite NA-oxide (NAO) by P450 enzymes is the key step in NA-induced cellular damage in airways (Warren *et al.*, 1982; Buckpitt and Warren, 1983). The reaction of NAO with reduced glutathione (GSH), to produce NA-glutathione conjugates (NA-GSH), is one of major detoxification pathways for the toxicant, and allows NA-GSH to serve as a marker of NA bioactivation in vitro and in vivo (Buckpitt *et al.*, 1984; Richieri and Buckpitt, 1988; Buckpitt *et al.*, 1992; Tingle *et al.*, 1993; Wilson *et al.*, 1996). Recent studies have provided further details on the involvement of P450 enzymes in NA bioactivation, including the respective roles of mouse CYP2A5 and CYP2F2 in mediating NA-induced nasal and lung toxicity (Li *et al.*, 2011; Hu *et al.*, 2014). The ability of human CYP2A13/CYP2F1 to bioactivate NA in vivo and mediate NA-induced acute nasal and lung toxicity at occupationally relevant inhalation exposure levels has also been demonstrated in a CYP2A13/CYP2F1-humanized mouse model (Li *et al.*, 2017). The latter study provides strong supporting evidence for the potential of NA to cause respiratory toxicity in humans.

The aim of this study was to determine whether a decrease in hepatic microsomal P450 activity would impact lung toxicity induced by inhalation exposure to NA; the answer to this question may impact human risk assessment for NA. We hypothesized that a decrease of P450 activity in liver, as would occur in people with liver diseases, will increase the amount of NA available for bioactivation by lung P450s, resulting in the formation of greater amounts of reactive metabolites and more severe damage to the pulmonary airways. The impact of the loss of hepatic NA metabolic activity on systemic NA clearance has been demonstrated previously in mice exposed to intraperitoneally injected NA at relatively high doses (Li *et al.*, 2011). However, the impact of hepatic metabolic disposition on the pharmacokinetics of NA may differ by exposure route; during an inhalation exposure, the respiratory tract would be exposed to NA delivered directly from the air and NA delivered through the blood circulation following absorption.

In the present study, we exposed mice to occupationally relevant doses (5 and 10 ppm) of NA through inhalation, and compared the pharmacokinetics of NA and NA-GSH, and the extent of NA-induced airway cytotoxicity, between wild-type (WT) and liver-Cpr-null

(LCN) mice. The LCN mice undergo tissue-specific deletion of the *Cpr* gene in all hepatocytes, which results in tissue-specific abolishment of microsomal P450 activities in the liver (Gu *et al.*, 2003a). Thus, we can determine whether a decrease in hepatic microsomal P450 activity would impact lung toxicity induced by inhalation exposure to NA. The LCN mouse model has been previously utilized to demonstrate the impact of hepatic P450-mediated NA metabolism on the pharmacokinetics of systemically administered NA (Li *et al.*, 2011).

Materials and Methods

Chemicals and reagents

NA (CAS# 91–20-3, purity 99%), NA-d_8 (CAS# 1146–65-2, purity 99%), GSH(CAS# 70–18-8, purity ≥ 98.0%), β-nicotinamide adenine dinucleotide phosphate, reduced tetra(cyclohexyl ammonium) salt (NADPH) (CAS#, 100929–71-3, purity ≥ 95.0%), and corn oil (highly refined, low acidity)were purchased from Sigma Aldrich (St. Louis, MO). Acetaminophen-glutathione (AP-GSH) was purchased from Toronto Research Chemicals (Toronto, ON, Canada). NA-GSH standard as a mixture of all four stereoisomers was a generous gift from Drs. Alan R. Buckpitt and Dexter Morin (University of California at Davis, Davis, CA) and was prepared as previously described (Richieri and Buckpitt, 1987a). All solvents (dichloromethane, formic acid, methanol and water) were of analytical grade (Fisher Scientific, Houston, TX). Ingredients for Karnovsky's fixative were from Tousimis (Rockville, MD).

In vitro assay of NA metabolism

Lung and liver microsomes were prepared from three different batches (each prepared from pooled tissue of 3 mice) of 2-month old, male, LCN and WT mice, as described (Gu *et al.*, 1998). In vitro assay of NA bioactivation was performed as described previously (Shultz *et al.*, 1999); reaction mixtures contained 50 mM phosphate buffer (pH 7.4), NA at a wide range of concentrations added in 2 μL of methanol (0; 0.5; 1.0; 2.0; 5.0; 10.0; 20.0; 50.0; 100.0; 200.0 and 400.0 μM), 10 mM GSH, 0.2 mg/ml of liver or lung microsomal protein, and 0 or 1.0 mM NADPH, in a final volume of 0.2 mL. The reaction was carried out at 37 ^{o}C in sealed tubes for 5 min and terminated by the addition of 2 volumes of ice-cold methanol containing 2.5 ng of AP-GSH (internal standard). The resultant mixtures were centrifuged to remove precipitated proteins, and NA-GSH was quantified in aliquots of the supernatant using LC-MS/MS (see below).

Animal experiments

All procedures involving animals were approved by the Wadsworth Center Institutional Animal Care and Use Committee. WT B6 and LCN (Gu *et al.*, 2003b) mice from colonies maintained at Wadsworth Center were housed in an acclimatized environment on a 12-h light:dark cycle, and had access to standard rodent chow and drinking water *ad libitum*. Two-month-old male mice were used for experiments.

Nose-only inhalation exposure to HEPA-filtered air (sham-exposure control) or NA vapor was conducted in an Oral Nasal Aerosol Respiratory Exposure System (equipped with a 24-

port Jaeger rodent inhalation exposure chamber) (CH Technologies, Westwood, NJ). Mice were acclimatized to the holding tube and exposure chamber (once a day for three days) prior to NA exposure. To generate NA vapor, air was passed through a glass column containing crystalline NA, heated to 52 °C; the vapor was mixed with fresh filtered air to achieve desired average NA concentration in the inhalation chamber. All experiments were started in the morning and consisted of two 2-h exposure periods with a 1-h break in between (added to reduce stress to mice). NA vapor at two different doses was studied, 5 and 10 ppm; the latter dose is an OSHA (http://www.osha.gov/dts/chemicalsampling/data/CH_255800.html) permissible exposure limit for human workers. The 4-h total exposure time was selected to mimic daily occupational exposure.

Concentrations of NA, carbon dioxide (CO_2), carbon monoxide (CO), and oxygen (O_2); relative humidity; and air temperature in the exposure chamber were monitored in real time throughout the exposure using a model IQ-604 Total Volatile Organic Compound (TVOC) Monitor (Graywolf Sensing Solutions, Trumbull, CT), which was pre-calibrated for NA as recently described (Li *et al.*, 2017). Air flow through each nose port was maintained at approximately 0.3 L/min.

For toxicokinetics studies, blood samples (~20 μL each) from individual mice were collected from the tail vein using heparinized capillary tubes at various time points (0–360 min) after termination of NA exposure. Plasma was prepared by centrifugation of blood samples at 10,000 rpm for 5 min at 4 °C, and was stored in sealed tubes at −80 °C until use. For detection of tissue levels of NA and NA-GSH, mice were placed in fresh air (immediately after termination of NA exposure) for 0, 2, 4 and 20 hours and then euthanized by CO_2 overdose. Lung (lavaged with 1 mL of 1X phosphate-buffered saline (PBS)) and liver were harvested, quick-frozen, and stored in sealed tubes at −80 °C until use.

NA and NA-GSH detection

For NA detection, plasma (10 μL) or tissue (lung, liver) homogenates (50 μL) were spiked with NA-d_8 (18 pg for plasma and 12 pg for tissue, in 10 μL of methanol), extracted with dichloromethane (100 μL for plasma and 110 μL for tissue). The organic phase (1 μL injection volume) was analyzed for NA using gas-chromatography mass spectrometry in a splitless injection mode, as previously described (Li *et al.*, 2011), using a Restek Rxi-5ms (30 m x 0.25 mm; 0.25 μm) column (Restek, Bellefonte, PA). The limit for NA detection was 0.8 pmol (on column).

For NA-GSH detection, plasma (10 μL) and tissue homogenate (50 μL) were spiked with an internal standard AP-GSH (2 ng in 10 μL of methanol), and then mixed with methanol (80 and 90 μL, respectively) for protein precipitation. An aliquot of the supernatant (1 μL) was analyzed for NA-GSH using liquid-chromatography mass spectrometry, with a SCIEX 4000 Q-Trap mass spectrometer, as previously described (Li *et al.*, 2011), or with a SCIEX 6500 Q-Trap mass spectrometer (AB-SCIEX, Framingham, MA), as described below.

The 6500 Q-Trap mass spectrometer was coupled to an Agilent 1290 Infinity Series ultra-performance liquid chromatography system (Agilent, Santa Clara, CA) and an Agilent Elipse Plus C18 (2.1 × 50 mm; 1.8 μm) column. Analytes were eluted at room temperature,

at a flow rate of 0.2 mL/min, with mobile phases as previously described (Li *et al.*, 2011), using the following program: linear increase from 10%B to 90%B from 0 to 4 min, return to 10%B from 4 to 8 min, and re-equilibration at 10%B for 2 min. The retention times of NA-GSH and AP-GSH were 2.9 and 2.3 min, respectively. The mass spectrometer was operated in positive ion mode using electrospray ionization with the following settings: ion spray voltage, 5500V; temperature, 500°C; curtain gas, 30 psi; ion source gas 1, 22 psi; ion source gas 2, 10 psi; declustering potential, 95 V; and entrance potential, 10 V. Analytes were detected using multiple reaction monitoring (MRM), with the following settings: dwell time, 125 ms; collision gas, medium; collision energy, 30 V; and collision cell exit potential, 10 V. The MRM transitions used for NA-GSH quantification and confirmation were 452/306 and 452/288, respectively. Quantification of the internal standard, AP-GSH, was done using the MRM transition 457/328. The limit for NA-GSH detection was 0.55 pmol (on column). All samples were analyzed in duplicate.

High-resolution histology and quantitative histopathology

Mice were exposed to HEPA-filtered air (FA) or NA vapor (5 or 10 ppm) as described above, and sacrificed 20 hours after termination of the exposure, by CO_2 overdose. The lungs were inflated with Karnovsky's solution as described previously (Van Winkle *et al.*, 2001; Van Winkle *et al.*, 2004; Van Winkle *et al.*, 2017). Fixed lung lobes were embedded in Araldite 502 resin. Lung sections (1-μm thick) were stained with methylene blue azure II. Proximal airways and terminal bronchioles were imaged on an Olympus BH-2 microscope using Adobe Photoshop image capture software. The morphometric procedures for detection of injured epithelial cells in different airway regions were performed as described elsewhere (Hyde *et al.*, 1990). The volume fractions (V_v) were defined by point (P) and intercept (I) counting using a cycloid grid and Stereology Toolbox (Morphometrix, Montpellier, France) for a minimum of 200 points. V_v was calculated using the formula $V_v = P_n/P_t$, where P_n is the number of test points hitting structures of interest (damaged epithelial cells), and P_t is the total points hitting the reference space (epithelial cells). Eight proximal bronchioles or distal airways (at a minimum) from each animal were used to determine morphometric parameters, which were used to calculate the mean and the standard deviation for each exposed group of animals per genotype.

Other methods and data analysis

The Michaelis-Menten kinetic parameters, *K*m and *V*max, for in vitro metabolism studies were calculated using GraphPad Prism (GraphPad, San Diego, CA). Student's t-test was used to analyze the differences between kinetic parameters. The delivered dose of inhaled NA following inhalation exposure was calculated per guidelines (Alexander *et al.*, 2008), using WinNonlin software (Pharsight, Mountain View, CA). Given that bioavailability (F) of NA is unknown after inhalation administration in mice, clearance (CL) was determined as a hybrid parameter CL/F. Data from multiple groups were compared using a two-way analysis of variance (ANOVA), followed by Bonferroni's test for multiple comparisons. $p<0.05$ was considered statistically significant.

Results

Liver-specific impact of hepatic cytochrome P450 reductase gene (*Cpr*) deletion on NA metabolism in vitro

NA metabolism by lung and liver microsomal preparations was compared between WT and LCN mice. The rates of formation of the reactive 1,2-NA epoxide were determined by measuring NA-GSH produced in the presence of added GSH. The rates of NA-GSH formation were linear with time under the conditions of the assay. As shown in Table 1, catalytic efficiency for the formation of NA-GSH, determined using a broad range of NA concentrations (0.5–400 μM) and saturating amounts of GSH, was 10-fold lower in the liver of LCN mice, compared to that in WT mice; but it was similar between the two mouse strains in the lung.

Impact of hepatic *Cpr* deletion on pharmacokinetics of plasma NA and NA-GSH following NA inhalation exposure

NA and NA-GSH were measured in the plasma of WT and LCN mice immediately following the inhalation exposure session (2 h NA, 1 h rest, 2 h NA). As shown in Figure 1, after a NA exposure at 10 ppm, the levels of NA and NA-GSH in the plasma of LCN mice were significantly higher than in WT mice at most time-points examined. Pharmacokinetic analysis of the data in Figure 1 indicated ~2-fold higher Cmax values for NA and ~2.5-fold higher Cmax values for NA-GSH in LCN than in WT mice. The AUC values for NA and NA-GSH were respectively ~2 and ~11 times greater in LCN compared to WT mice (Table 2). The rate of NA clearance (Cl/F) in LCN mice was one-half of that in WT mice, coupled with an increased (by ~1.4 fold) plasma elimination half-life ($t_{1/2}$). These results indicate that the loss of hepatic P450 activity led to increases in systemic bioavailability of inhaled NA. However, the plasma level of NA-GSH was not decreased; in contrast, it was dramatically increased in the LCN mice.

Impact of hepatic *Cpr* deletion on NA and NA-GSH levels in lung and liver following NA inhalation exposure

Levels of NA were determined in target (lung) and non-target (liver) tissues of WT and LCN mice exposed to 5 or 10 ppm of NA vapors. NA was detected in lungs of WT and LCN mice immediately after termination of NA exposure, but it was not detected at other time points examined (2, 4 and 20 hours) (Fig. 2A), with an estimated detection limit of ~4.5 ng of NA/g tissue. NA levels in the lungs of LCN mice were higher than in WT mice, at the “0-h” time point, for the 10-ppm (by >5-fold, $p < 0.0001$) NA dose, with the levels in the 10-ppm NA exposed LCN mice significantly higher (by >3-fold, $p < 0.0001$) than in the 5-ppm NA exposed LCN mice. NA levels in the lungs of LCN mice also appeared to be higher than in WT mice for the 5-ppm NA dose (by >3-fold), though the difference did not reach statistical significance.

NA was not detected in the livers of WT mice regardless of the NA dose and postexposure time. However, the livers of LCN mice exposed to 5-ppm NA had relatively low, but quantifiable amounts of NA at early time points (0–4 h), whereas those LCN mice exposed to 10-ppm NA had significantly greater amounts of NA (>7-fold, vs the 5-ppm group, p <

0.0001) in their livers at those same time points (Fig. 2B). NA was no longer detectable at the 20-h time point, for either NA dose. NA was not detected in any tissue samples from sham (FA)-exposed WT or LCN mice (data not shown).

NA-GSH was detected in lung (Fig. 2C) and liver (Fig. 2D) of WT and LCN mice at the early (0-h, 2-h and most 4-h) time points after inhalation of 5 or 10 ppm NA vapors, and in the late (20 h) time point after exposure to the high NA dose (10 ppm). NA-GSH levels varied in lungs and livers of WT mice at dose- and time-dependent fashion. Remarkably, NA-GSH levels were elevated in both lung and liver of LCN mice, compared to WT mice, at 2 or 4 h after termination of NA exposure (at 10 ppm, $p < 0.0001$). A trend of increase was also observed for the same comparisons at 5 ppm. In contrast to the rapid postexposure decline in tissue NA-GSH levels seen in the WT mice, the rates of decline in the LCN mice were much lower. Additionally, NA-GSH levels were generally higher in the liver than in the lungs of the same animals, at each time point. NA-GSH was not detected in any tissue samples from FA-exposed WT or LCN mice (data not shown).

Impact of hepatic *Cpr* deletion on the extents of tissue injury induced by inhaled NA in the airways

NA-induced damage to airway epithelial cells of WT and LCN mice was evaluated at 20 h after termination of exposure, via high-resolution microscopy and quantitative morphometry (Van Winkle *et al.*, 1995). The relative abundance of cytotoxic cells, which show vacuolization, swelling, and/or partial detachment from the basal lamina (Fig. 3A, 3B), is measured as fraction of damaged cells among total epithelial cells, represented by the parameter “volume fraction” (Vv), which is shown in Figure 3C for all treatment groups. NA exposure at either 5 or 10 ppm caused significant increases in the fraction of damaged epithelial cells compared to the FA-treated control groups ($p<0.0001$), in both proximal and distal airways, with no obvious difference between NA exposure groups or airway regions. However, the fraction of damaged epithelial cells was substantially lower in the LCN mice than in the WT mice (by 36% and 39% in the proximal and distal airways, respectively, at 10 ppm, $p<0.01$, and by 22% ($p=0.12$) and 29% ($P<0.05$) in the proximal and distal airways, respectively, at 5 ppm). Notably, there were no differences in the average total airway thickness among all groups (not shown).

Discussion

The impact of hepatic P450-mediated NA metabolism on airway toxicity of NA in an inhalation exposure scenario may include effects on tissue burdens of NA and potentially toxic NA metabolites in the lung and airways (Fig. 4). During NA inhalation, the airway epithelial cells are exposed simultaneously to NA aerosols in the airway and NA and NA metabolites arriving from systemic circulation. NA in systemic circulation can be transported to the airway epithelial cells to undergo target tissue bioactivation and cause cytotoxicity, as demonstrated by the induction of airway cytotoxicity following intraperitoneal NA administration and by vascular perfusion of the lung with NAO (Plopper *et al.*, 1992b). Similarly, NA metabolites, such as NAO, can cause airway Club cell toxicity when administered by vascular perfusion of the isolated lung or in vitro (Kanekal S, 1991;

Chichester *et al.*, 1994). However, the sizes of the two pools of NA and of NA metabolites, and their relative contributions to the airway toxicity of inhaled NA, are currently unknown.

Our finding that suppression of hepatic P450 activity can lead to increased bioavailability of inhaled NA in the lung is not unexpected, although experimental confirmation was necessary and the determination of the extent of the increased bioavailability is important for interpreting results of subsequent toxicity study. However, despite the substantial increase in circulating and lung tissue NA levels (Fig. 1 and 2), the extent of NA-induced acute airway injury, judging from lung histopathology at 20 h following NA exposure, was lower in LCN than in WT mice (Fig. 3). This finding is consistent with the pharmacokinetics of NA-GSH, a biomarker of NA bioactivation. In that regard, the steady-state levels of lung NA-GSH at the termination of the 10-ppm NA exposure ("0" hour) were only slightly higher in LCN than in WT mice, but the difference in the apparent half-life was much more noteworthy (Fig. 2C). That observation has two implications. One, regarding steady-state NA levels during active exposure, is that the lung tissue levels of NA and circulating levels of NA do not seem to directly translate to levels in airway epithelial cells, which may have a slow extraction of "blood-borne" NA, which may be bound to serum proteins, relative to the rapid absorption of airborne NA. Two, regarding NA bioactivation, is that the greater blood and lung tissue levels of NA do appear to translate to a more sustained exposure of the airway cells to systemically derived NA, and to greater participation of airway cells in NA bioactivation in the lung, following the termination of active exposure.

Notably, NA-GSH is one of several proximal metabolites of the reactive NAO. The others include 1-naphthol, NA-protein adducts, and NA conjugates with other non-protein thiols. The relative abundance of NA-GSH to these other NAO metabolites may be influenced by the availability of GSH, leading to discordance in the levels of NA-GSH detected and the amounts of NAO generated. However, plasma levels of NA and NA-GSH were increased in parallel in the LCN mice, relative to WT mice (Fig. 1), indicating that GSH levels were not a limiting factor in NA-GSH formation in this study. Furthermore, there was no significant difference in lung total non-protein thiol levels between WT and LCN mice at the termination of exposure to 5 ppm NA (data not shown). Thus, GSH limitation is unlikely the explanation for the data showing that, while there were substantial differences in the levels of NA in WT and LCN mice, there was virtually no strain-related difference in NA-GSH levels in the livers or lungs of these animals at the end of the NA active exposure period (Fig. 2).

Our present finding, that the LCN mouse did not show greater toxicity than WT mice following inhalation exposure to NA, may be explained in part by the low abundance of NA available from the circulation under the occupationally relevant exposure conditions of the present study, relative to NA exposure from the air. The highest levels of NA reached in circulation following inhalation exposure to NA at 10 ppm (<100 ng/ml in WT mice; <200 ng/ml in LCN mice; this study) may be too low to make a notable contribution to lung airway toxicity, compared to levels reached following intraperitoneal injection of NA at a toxic, 300 mg/kg, dose (Cmax at 3–4 μg/ml in WT mice and almost 20 μg/ml in LCN mice) (Li *et al.*, 2011).

On the other hand, the small but significant decrease in LCN vs WT mice in the extent of airway cytotoxicity (Fig. 3) suggests a small but definitive contribution by hepatic P450 bioactivation to airway toxicity by inhaled NA. In that regard, previous studies have shown that NAO, the obligatory reactive intermediate of NA, formed intracellularly by isolated mouse hepatocytes, was able to diffuse from cells (Richieri and Buckpitt, 1987b), and cause vacuolization, necrosis and exfoliation of nonciliated bronchiolar epithelial cells in isolated, perfused mouse lung (Kanekal S, 1991). Liver-generated NAO is theoretically stable enough (e.g., $t_{1/2}$ was 10 min in both whole blood and plasma under in vitro conditions) (van Bladeren *et al.*, 1984; Kanekal S, 1991; Tsuruda *et al.*, 1995) to circulate to the lung and cause damage. It remains to be directly confirmed whether loss of hepatic NA bioactivation leads to significant decreases in circulating or lung tissue levels of these metabolites; but our present data seem to support this notion.

Two different concentrations of NA (5 and 10 ppm) were studied. A dose-response relationship was found in lung NA and NA-GSH levels, with greater tissue burdens found for the higher NA concentration (Fig. 2). Curiously, a dose response was not observed for the cytotoxicity index (Fig. 3). It seems unlikely that the NA concentrations employed are already saturating, as there was a clear, dose-dependent increase in bioactivation in vivo (NA-GSH formation). One possible explanation for this observation is that the higher concentration caused more rapid cell death during the active exposure, but the method that we used to determine cell injury does not reveal how rapidly the cells were killed. Alternatively, the airway cells that had died prior to the 20 h time point did not contribute to the Vv(damaged) values, thus making it appear that the two concentrations resulted in a similar extent of tissue injury. A detailed time course study would be needed to detect a dose-related difference in rates of NA-induced cell death. However, the comparison of cytotoxicity between WT and LCN mice at the 10-ppm concentration is unlikely influenced by a possible difference in rates of cell death, as, unlike the concentration comparisons, the two genotype groups had only slightly different levels of NA-GSH (a biomarker of in vivo bioactivation) at the termination of exposure (Fig. 2C).

The pharmacokinetics data for plasma NA-GSH following inhalation exposure to NA (Fig. 1B, Table 2) differ from previous results with intraperitoneal NA injection, where similar AUC and Cmax values were found between WT and LCN mice; but the T_{max} value was slightly increased, probably reflecting the need for NA to accumulate in the lungs before metabolism can occur at a maximal rate, in the LCN mice (Li *et al.*, 2011). In the inhalation exposure model, we could not determine T_{max}, or whether a shift in T_{max} occurred, but we found that both Cmax and AUC values are greater in LCN than in WT mice (Table 2). This increase in NA-GSH level may reflect the pool of NA-GSH produced by lung and other extrahepatic organs, such as the nasal mucosa, from blood-borne NA (which is much increased in LCN mice) in addition to the pool of NA-GSH formed by lung and nasal mucosa from air-borne NA during first-pass NA metabolism in the airway. Thus, inhaled NA and injected NA are both still efficiently bioactivated in vivo in the absence of significant contribution by hepatic microsomal P450s. Notably, the relative contributions of various extrahepatic tissues to circulating NA-GSH in the LCN mice remain to be determined. For the nasal olfactory mucosa, which contains abundant NA-bioactivating P450 enzymes (CYP2A5 and CYP2F2) (Hu et al., 2014), it will be interesting to determine whether the

bulk of the produced NA-GSH is excreted to the circulation (thus contributing to plasma levels of NA-GSH) or to the nasal mucus. Additionally, while the data in Figure 1B does not reveal whether the rate of NA-GSH degradation was different between WT and LCN mice, the previous pharmacokinetic data for NA-GSH in LCN mice exposed to NA via the intraperitoneal route (Li et al., 2011) argues against such a possibility. Thus, the apparent persistence of NA-GSH in the plasma of LCN mice after termination of NA inhalation exposure was probably mainly due to continued NA metabolism and NA-GSH formation during the post exposure period.

NA-GSH was present in the liver as well as in the lung, in both WT and LCN mice, although the latter mouse could not produce significant amounts of NA-GSH in the liver via P450-mediated pathways. It is unlikely that the hepatic NA-GSH was produced in the liver by a non-CYP pathway, as a previous study with *Cyp2f2*-null mice showed that in vivo formation of NA-GSH is largely P450-dependent (Li *et al.*, 2011). Thus, the hepatic NA-GSH must have been produced in the lung and other extrahepatic tissues and then transported to the liver, in the LCN mice.

In conclusion, hepatic microsomal P450 enzymes are not essential for induction of airway toxicity by inhaled NA. Furthermore, although hepatic P450-mediated systemic clearance of inhaled NA had a significant impact on NA levels in the lung and plasma, the increase in lung NA levels because of a functional deficiency of hepatic P450 enzymes did not noticeably impact the extent of NA-induced airway toxicity, at least under the low-dose occupational exposure conditions employed and at the postexposure time point examined here. Conversely, our data further suggest that liver P450-generated NA metabolites have a relatively small, but significant, contribution to airway toxicity of inhaled NA. This hepatic contribution to the airway toxicity of inhaled NA may be an important risk factor for individuals with diminished bioactivation activity in the lung.

Acknowledgments

We gratefully acknowledge the use of the services of the Pathology Core and the Advanced Light Microscopy and Image Analysis Core Facilities of the Wadsworth Center. We thank Ms. Weizhu Yang for assistance with mouse breeding.

Funding

This study was supported in part by grant ES020867 and ES023513 from the National Institute of Environmental Health Sciences, NIH.

ABBREVIATIONS:

NA	naphthalene
NAO	naphthalene oxide
Cpr	cytochrome P450 reductase
LCN	liver-Cpr-null
WT	wild-type

GSH	glutathione
NADPH	β-nicotinamide adenine dinucleotide phosphate
AP-GSH	acetaminophen-glutathione conjugate
NA-GSH	naphthalene-glutathione conjugate
PBS	phosphate-buffered saline
F	bioavailability
CL	clearance
$t_{1/2}$	elimination half-life
FA	filtered air

References:

Abdo KM, Eustis S, McDonald M, Jokinen M, Adkins B, Haseman J, 1992 Naphthalene: A respiratory tract toxicant and carcinogen for mice. Inhal Toxicol 4, 393–409.

Abdo KM, Grumbein S, Chou BJ, Herbert R, 2001 Toxicity and carcinogenicity study in F344 rats following 2 years of whole-body exposure to naphthalene vapors. Inhal Toxicol 13, 931–950. [PubMed: 11696867]

Alexander DJ, Collins CJ, Coombs DW, Gilkison IS, Hardy CJ, Healey G, Karantabias G, Johnson N, Karlsson A, Kilgour JD, McDonald P, 2008 Association of Inhalation Toxicologists (AIT) working party recommendation for standard delivered dose calculation and expression in non-clinical aerosol inhalation toxicology studies with pharmaceuticals. Inhal Toxicol 20, 1179–1189. [PubMed: 18802802]

Brusick D, 2008 Critical assessment of the genetic toxicity of naphthalene. Regul Toxicol Pharmacol 51, S37–42.

Buckpitt A, Boland B, Isbell M, Morin D, Shultz M, Baldwin R, Chan K, Karlsson A, Lin C, Taff A, West J, Fanucchi M, Van Winkle L, Plopper C, 2002 Naphthalene-induced respiratory tract toxicity: metabolic mechanisms of toxicity. Drug Metab Rev 34, 791–820. [PubMed: 12487150]

Buckpitt A, Buonarati M, Avey LB, Chang AM, Morin D, Plopper CG, 1992 Relationship of cytochrome P450 activity to Clara cell cytotoxicity. II. Comparison of stereoselectivity of naphthalene epoxidation in lung and nasal mucosa of mouse, hamster, rat and rhesus monkey. J Pharmacol Exp Ther 261, 364–372. [PubMed: 1560380]

Buckpitt AR, Bahnson LS, Franklin RB, 1984 Hepatic and pulmonary microsomal metabolism of naphthalene to glutathione adducts: factors affecting the relative rates of conjugate formation. J Pharmacol Exp Ther 231, 291–300. [PubMed: 6491983]

Buckpitt AR, Warren DL, 1983 Evidence for hepatic formation, export and covalent binding of reactive naphthalene metabolites in extrahepatic tissues in vivo. J Pharmacol Exp Ther 225, 8–16. [PubMed: 6834280]

Chichester CH, Buckpitt AR, Chang A, Plopper CG, 1994 Metabolism and cytotoxicity of naphthalene and its metabolites in isolated murine Clara cells. Mol Pharmacol 45, 664–672. [PubMed: 8183245]

Gu J, Weng Y, Zhang Q-Y, Cui H, Behr M, Wu L, Yang W, Zhang L, Ding X, 2003a Liver-specific Deletion of the NADPH-Cytochrome P450 Reductase Gene: impact on plasma cholesterol homeostasis and the function and regulation of microsomal cytochrome P450 and heme oxygenase. J Biol Chem 278, 25895–25901. [PubMed: 12697746]

Gu J, Weng Y, Zhang Q-Y, Cui H, Behr M, Wu L, Yang W, Zhang L, Ding X, 2003b Liver-specific Deletion of the NADPH-Cytochrome P450 Reductase Gene: impact on plasma cholesterol homeostasis and the function and regulation of microsomal cytochrome P450 and heme oxygenase. J Biol Chem 278, 25895–25901. [PubMed: 12697746]

Gu J, Zhang Q-Y, Genter MB, Lipinskas TW, Negishi M, Nebert DW, Ding X, 1998 Purification and characterization of heterologously expressed mouse CYP2A5 and CYP2G1: role in metabolic activation of acetaminophen and 2, 6-dichlorobenzonitrile in mouse olfactory mucosal microsomes. J Pharmacol Exp Ther 285, 1287–1295. [PubMed: 9618435]

Hu J, Sheng L, Li L, Zhou X, Xie F, D'Agostino J, Li Y, Ding X, 2014 Essential role of the cytochrome P450 enzyme CYP2A5 in olfactory mucosal toxicity of naphthalene. Drug Metab Dispos 42, 23–27. [PubMed: 24104196]

Hyde DM, Plopper CG, St George JA, Harkema JR, 1990 Morphometric cell biology of air space epithelium, Dekker, New York.

IARC, 2002 Traditional herbal medicines, some mycotoxins, naphthalene and styrene. IARC Monographs On the Evaluation of Carcinogenic Risks to Humans 82, 1–601. [PubMed: 12687954]

Kakareka SV, Kukharchyk TI, 2003 PAH emission from the open burning of agricultural debris. Sci Total Environ 308, 257–261. [PubMed: 12738218]

Kanekal S PC, Morin D, Buckpitt A, 1991 Metabolism and cytotoxicity of naphthalene oxide in the isolated perfused mouse lung. J Pharmacol Exp Ther 256, 391–401. [PubMed: 1988668]

Li L, Carratt S, Hartog M, Kovalchuk N, Jia K, Wang Y, Zhang Q, Edwards PC, Van Winkle LS, Ding X, 2017 Human CYP2A13 and CYP2F1 mediate naphthalene toxicity in the lung and nasal mucosa of CYP2A13/2F1-humanized mice. Environ Health Perspect in press.

Li L, Wei Y, Van Winkle LS, Zhang Q-Y, Zhou X, Hu J, Xie F, Kluetzman K, Ding X, 2011 Generation and characterization of a Cyp2f2-null mouse and studies on the role of CYP2F2 in naphthalene-induced toxicity in the lung and nasal olfactory mucosa. The J Pharmacol Exp Ther 339, 62–71. [PubMed: 21730012]

Plopper CG, Macklin J, Nishio SJ, Hyde DM, Buckpitt AR, 1992a Relationship of cytochrome P-450 activity to Clara cell cytotoxicity. III. Morphometric comparison of changes in the epithelial populations of terminal bronchioles and lobar bronchi in mice, hamsters, and rats after parenteral administration of naphthalene. Lab Invest 67, 553–565. [PubMed: 1434534]

Plopper CG, Suverkropp C, Morin D, Nishio S, Buckpitt AR, 1992b Relationship of cytochrome P-450 activity to Clara cell cytotoxicity. I. Histopathologic comparison of the respiratory tract of mice, rats and hamsters after parenteral administration of naphthalene. J Pharmacol Exp Ther 261, 353–363. [PubMed: 1560379]

Richieri PR, Buckpitt AR, 1987a Efflux of naphthalene oxide and reactive naphthalene metabolites from isolated hepatocytes. J Pharmacol Exp Ther 242, 485–492. [PubMed: 3612547]

Richieri PR, Buckpitt AR, 1987b Efflux of naphthalene oxide and reactive naphthalene metabolites from isolated hepatocytes. J Pharmacol Exp Ther 242, 485–492. [PubMed: 3612547]

Richieri PR, Buckpitt AR, 1988 Glutathione depletion by naphthalene in isolated hepatocytes and by naphthalene oxide in vivo. Biochem Pharmacol 37, 2473–2478. [PubMed: 3390209]

Shultz MA, Choudary PV, Buckpitt AR, 1999 Role of murine cytochrome P-450 2F2 in metabolic activation of naphthalene and metabolism of other xenobiotics. J Pharmacol Exp Ther 290, 281–288. [PubMed: 10381788]

Tingle MD, Pirmohamed M, Templeton E, Wilson AS, Madden S, Kitteringham NR, Park BK, 1993 An investigation of the formation of cytotoxic, genotoxic, protein-reactive and stable metabolites from naphthalene by human liver microsomes. Biochem Pharmacol 46, 1529–1538. [PubMed: 8240407]

Tsuruda LS, Lame MW, Jones AD, 1995 Formation of epoxide and quinone protein adducts in B6C3F1 mice treated with naphthalene, sulfate conjugate of 1,4-dihydroxynaphthalene and 1,4-naphthoquinone. Arch Toxicol 69, 362–367. [PubMed: 7495373]

USEPA, 1986 Summary of Emissions Associated with Sources of Naphthalene.

van Bladeren PJ, Vyas KP, Sayer JM, Ryan DE, Thomas PE, Levin W, Jerina DM, 1984 Stereoselectivity of cytochrome P-450c in the formation of naphthalene and anthracene 1,2-oxides. J Biol Chem 259, 8966–8973. [PubMed: 6430894]

Van Winkle LS, Brown CD, Shimizu JA, Gunderson AD, Evans MJ, Plopper CG, 2004 Impaired recovery from naphthalene-induced bronchiolar epithelial injury in mice exposed to aged and diluted sidestream cigarette smoke. Toxicol Lett 154, 1–9. [PubMed: 15475173]

Van Winkle LS, Buckpitt AR, Nishio SJ, Isaac JM, Plopper CG, 1995 Cellular response in naphthalene-induced Clara cell injury and bronchiolar epithelial repair in mice. Am J Physiol 269, L800–L818. [PubMed: 8572242]

Van Winkle LS, Evans MJ, Brown CD, Willits NH, Pinkerton KE, Plopper CG, 2001 Prior exposure to aged and diluted sidestream cigarette smoke impairs bronchiolar injury and repair. Tox Sci 60, 152–164.

Van Winkle LS, Kelty JS, Plopper CG, 2017 Preparation of Specific Compartments of the Lungs for Pathologic and Biochemical Analysis of Toxicologic Responses. Curr Protoc Toxicol 71, 24 25 21–24 25 26. [PubMed: 28146282]

Warren DL, Brown DL, Jr., Buckpitt AR, 1982 Evidence for cytochrome P-450 mediated metabolism in the bronchiolar damage by naphthalene. Chem Biol Interact 40, 287–303. [PubMed: 7083396]

West JA, Pakehham G, Morin D, Fleschner CA, Buckpitt AR, Plopper CG, 2001 Inhaled naphthalene causes dose dependent Clara cell cytotoxicity in mice but not in rats. Toxicol Appl Pharmacol 173, 114–119. [PubMed: 11384213]

Wilson AS, Davis CD, Williams DP, Buckpitt AR, Pirmohamed M, Park BK, 1996 Characterisation of the toxic metabolite(s) of naphthalene. Toxicol 114, 233–242.

Witschi H, Espiritu I, Maronpot RR, Pinkerton KE, Jones AD, 1997 The carcinogenic potential of the gas phase of environmental tobacco smoke. Carcinogenesis 18, 2035–2042. [PubMed: 9395199]

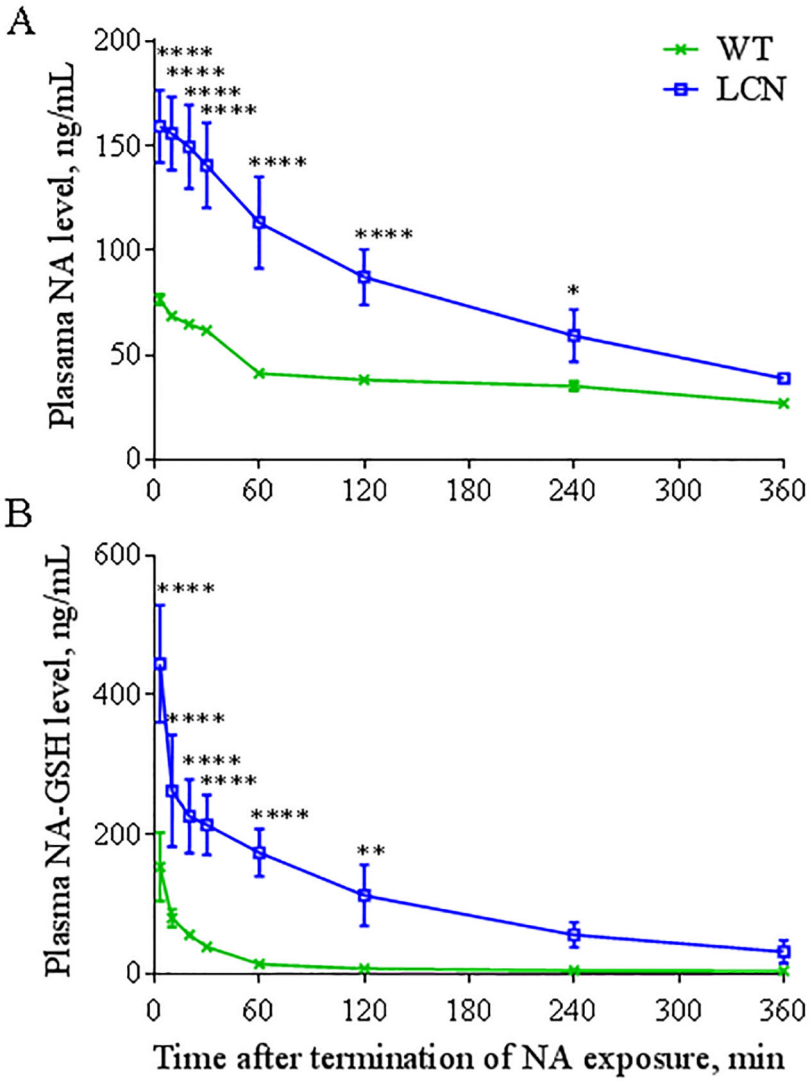

Fig. 1. Systemic level of NA and NA-GSH.

Two-month old wild-type (WT) and liver-Cpr-null (LCN) male mice were exposed to 10 ppm of naphthalene (NA) for 4 hours and plasma levels of NA (A) and naphthalene-glutathione conjugate (NA-GSH) (B) were determined at different time points after termination of NA exposure. Data represent means ± SD (n=4). *, **, ****, $p<0.05$, 0.01, or 0.0001, respectively, compared to WT mice (two-way ANOVA followed by Bonferroni's test for multiple comparisons).

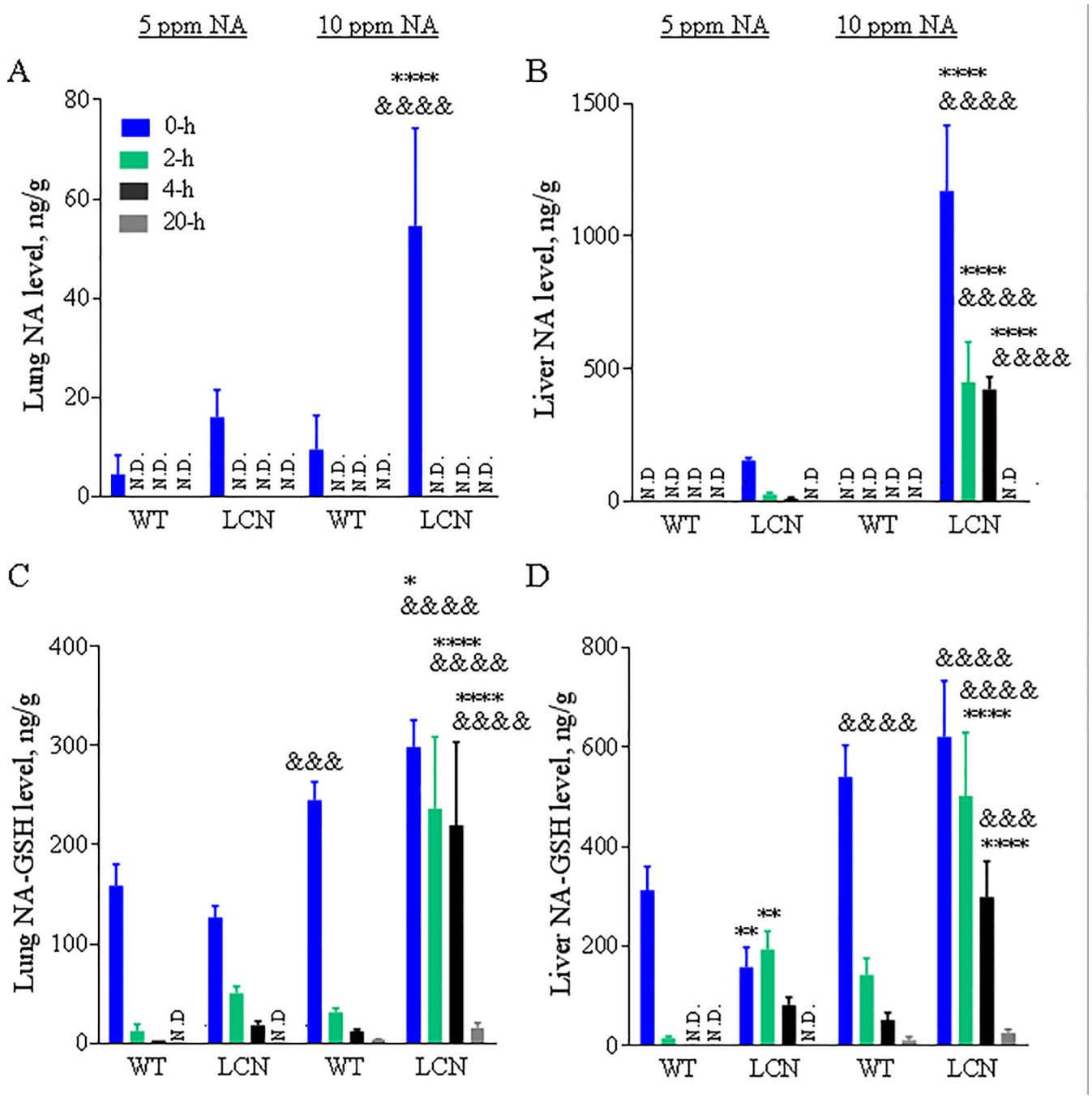

Fig. 2. NA and NA-GSH levels in mouse lung and liver after a single 4-hour nose-only inhalation exposure to different doses of NA.

Two-month old wild-type (WT) and liver-Cpr-null (LCN) male mice were exposed to 5 or 10 ppm of naphthalene (NA) for 4 h. Lung (A, C) and liver (B, D) were collected 0, 2, 4 and 20 hours after termination of NA exposure. NA (A, B) and naphthalene-glutathione conjugate (NA-GSH) (C, D) were detected in tissue homogenates. Data represent means ± SD (n=3–5). ****, $p<0.0001$; *, $p<0.05$; vs WT, of corresponding dose/time point; &&&&, $p<0.0001$; &&&, $p<0.001$; vs 5 ppm, of corresponding genotype/time point (two-way ANOVA followed by Bonferroni's test for multiple comparisons).

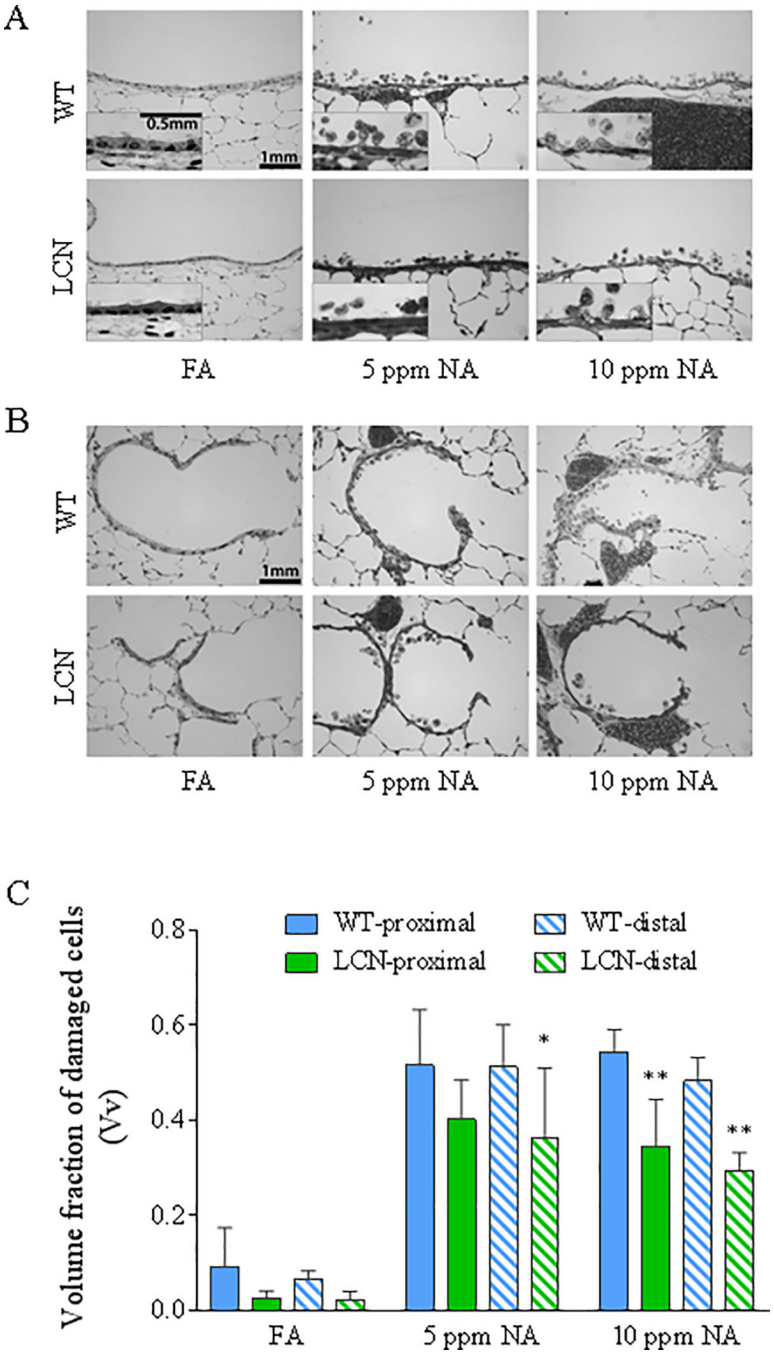

Fig. 3. High-resolution histologic analysis of the extent of airway epithelial damage induced by NA inhalation exposure in WT and LCN mice.

Two-month old wild-type (WT) and liver-Cpr-null (LCN) male mice were exposed to 5 or 10 ppm of naphthalene (NA), or to filtered air (FA), for 4 h. Mice were euthanized 20 h after termination of exposure, and lungs were processed for histopathologic analysis as described in Materials and Methods. (A, B) Typical signs of NA-induced epithelial Club cell damage, swelling, vacuolization, and exfoliation in the proximal bronchiole (A) and distal/terminal bronchiolar airways (B), as compared to the normal structures in FA-exposed control mice. Inset in A: enlarged views of swollen cells with darker nuclei staining, which signals cell

death, and intracellular vacuoles. Bar = 1 mm. (C), Results of blinded quantitative analysis of the extent of cellular injury in the various groups. The volume fractions (Vv) of damaged epithelial cells are shown as means ± S.D. (n =5 for NA-exposed groups, n=4–7 for FA-exposed groups). Vv was calculated as described in Materials and Methods. All NA-treated samples show significant increase over corresponding FA samples (all $p<0.0001$; not labeled); *, **, $p<0.05$ and $p<0.01$, respectively, significant difference by genotype (LCN vs WT) (two-way ANOVA, followed by Bonferroni's multiple comparisons test).

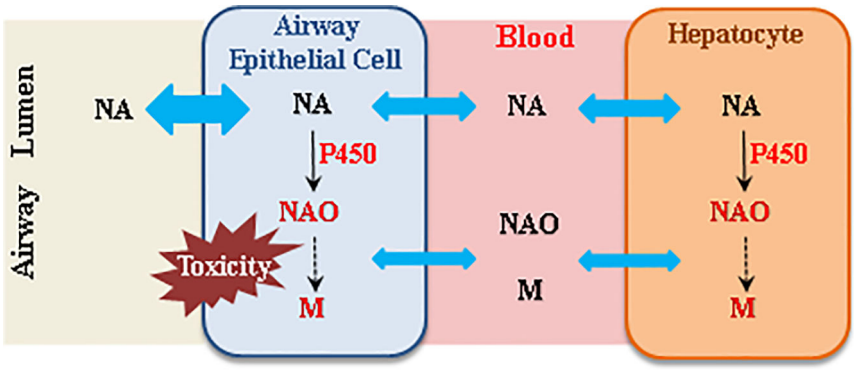

Fig. 4. Schematic representation of the potential impact of hepatic P450-mediated NA metabolism on airway toxicity of NA in an inhalation exposure scenario.

During inhalation naphthalene (NA) exposure, the airway epithelial cells are exposed simultaneously to NA aerosols in the airway, and NA, naphthalene oxide (NAO), and other NA metabolites (M) arriving from systemic circulation. Blue double arrow represents diffusion of NA into cells. Both “air-borne” NA and “blood-borne” NA can undergo target tissue bioactivation and cause cytotoxicity, whereas circulating NA metabolites, such as NAO, can also cause airway toxicity. However, the relative contributions of the various sources of reactive NA metabolites to airway toxicity are currently unknown.

Table 1

Enzyme kinetic parameters for the formation of NA-GSH from NA by lung and liver microsomes from WT and LCN mice

Apparent *Km* and *Vmax* values for the microsomal formation of NA-GSH were determined as described in *Methods*. The results shown represent means ± S.D. of values determined for three separate microsomal samples, each prepared from tissues pooled from three 2-month-old male mice.

Tissue, strain	Km, μM	Vmax, nmol/min/mg of protein	Vmax/Km, ml/mg of protein/min
Liver			
WT	4.71±0.76	1.10±0.04	0.23
LCN	5.09±0.89	0.12±0.01*	0.02
Lung			
WT	13.6±1.6	1.35±0.05	0.10
LCN	8.96±1.17	1.27±0.04	0.14

* $p<0.01$ (Student's t-test) compared to WT mice

Table 2

Pharmacokinetic parameters of NA and NA-GSH in the plasma of WT and LCN mice after NA inhalation exposure at 10 ppm

Values were derived from data presented in Figure 1.

Analyte, strain	AUC_{0-6h}, μg/ml/min	$t_{1/2}$, min	CL/F, ml/min	Cmax, ng/ml
NA				
WT	13.2±1.8	111±7	15.8±1.3	76.5±2.6
LCN	28.6 ±4.5 *	158±16 *	7.9±1.5 *	159±17 *
NA-GSH				
WT	3.0±0.2	N/A	N/A	153±49
LCN	33.6±10.5 *	N/A	N/A	445±84 *

* $p<0.01$ (Student's t-test), compared to corresponding WT mice

N/A, not applicable